

Special Paper

The Subsurface Geology of Río Tinto: Material Examined During a Simulated Mars Drilling Mission for the Mars Astrobiology Research and Technology Experiment (MARTE)

Olga Prieto-Ballesteros,¹ Jesús Martínez-Frías,¹ John Schutt,² Brad Sutter,³ Jennifer L. Heldmann,⁴ Mary Sue Bell,⁵ Melissa Battler,^{6,*} Howard Cannon,⁴ Javier Gómez-Elvira,¹ and Carol R. Stoker⁴

Abstract

The 2005 Mars Astrobiology Research and Technology Experiment (MARTE) project conducted a simulated 1-month Mars drilling mission in the Río Tinto district, Spain. Dry robotic drilling, core sampling, and biological and geological analytical technologies were collectively tested for the first time for potential use on Mars. Drilling and subsurface sampling and analytical technologies are being explored for Mars because the subsurface is the most likely place to find life on Mars. The objectives of this work are to describe drilling, sampling, and analytical procedures; present the geological analysis of core and borehole material; and examine lessons learned from the drilling simulation. Drilling occurred at an undisclosed location, causing the science team to rely only on mission data for geological and biological interpretations. Core and borehole imaging was used for micromorphological analysis of rock, targeting rock for biological analysis, and making decisions regarding the next day's drilling operations. Drilling reached 606 cm depth into poorly consolidated gossan that allowed only 35% of core recovery and contributed to borehole wall failure during drilling. Core material containing any indication of biology was sampled and analyzed in more detail for its confirmation. Despite the poorly consolidated nature of the subsurface gossan, dry drilling was able to retrieve useful core material for geological and biological analysis. Lessons learned from this drilling simulation can guide the development of dry drilling and subsurface geological and biological analytical technologies for future Mars drilling missions. **Key words:** Mars—Río Tinto—Iron oxides—Drilling core—Remote mineralogical analysis. *Astrobiology* 8, 1013–1021.

Introduction

THE MARS ASTROBIOLOGY RESEARCH AND TECHNOLOGY EXPERIMENT (MARTE) is a collaborative project between Centro de Astrobiología (CAB) (Spain) and NASA Ames Research Center (USA). The MARTE project is studying the subsurface biosphere in the Río Tinto region of Spain as a

potential biological and geological Mars analogue and is testing new drilling technologies for a future Mars mission. Searching for evidence of past life on Mars may require drilling into the subsurface to obtain biological evidence that is protected from the harsh oxidizing surface (Klein, 1979; Zent and McKay, 1994). The MARTE project is testing new robotic dry drilling, sample handling, and biological-geo-

¹Centro de Astrobiología (INTA-CSIC), Torrejón de Ardoz, Madrid, Spain.

²Mars Institute, NASA Research Park, Moffett Field, California.

³SETI Institute, Mountain View, California.

⁴NASA Ames Research Center, Moffett Field, California.

⁵Johnson Space Center, NASA, Houston, Texas.

⁶University of New Brunswick, Fredericton, Canada.

*Present address: University of Western Ontario, Centre for Planetary Science & Exploration, London, Ontario, Canada.

logical analysis technology that can provide access and analysis of the martian subsurface material.

The Río Tinto (Huelva, Spain) area was selected as the MARTE test site because it contains Fe mineralogies, such as iron oxides and sulfates, similar to those believed to be found on Mars. The Río Tinto Fe mineralogy also possesses biota that could be relevant to Mars (Fernández-Remolar *et al.*, 2003, 2004, 2005, 2008). The Río Tinto area is in the Iberian pyrite belt (Late Devonian to Mississippian of age), which hosts some of the world's largest volcanogenic massive sulfide ore deposits (Leistel *et al.*, 1998). Extraction of minerals has been conducted at least since the Bronze Age. The sulfide ore bodies are stratiform, sheetlike bodies within the Volcano-Sedimentary Complex, which overlies the Phyllite-Quartzite Group and in turn is overlain by the Culm Group shales (Moreno, 1993). The sulfide ores often exhibit sedimentary features and textures indicative of deposition on the sea floor (Tornos, 2006). The Volcano-Sedimentary Complex includes bimodal volcanic rocks—from basaltic lavas to silica-rich volcanoclastic units. The volcanic rocks are present as sills, dikes, and peperitic intrusions (brecciated volcanic material in marine sedimentary rock) including local hydrovolcanic eruption with associated breccias and debris-flow deposits. The sulfide deposits mostly overlie the felsic volcanics or are associated with shales. The massive sulfide lenses generally have quartz-rich sulfide stockwork feeder systems at their base. In cases where the footwall is composed of volcanic rocks, hydrothermal alteration such as seritization and chloritization are evident (Leistel *et al.*, 1998; Boulter *et al.*, 2004).

Alteration of the sulfides produces sulfates, iron oxides, and oxyhydroxide minerals. Sulfuric acid released in the oxidation process leads to heavy acidification of the aquifers and the formation of complex iron sulfate ions, which are the source of the eye-catching red river water (Fernández-Remolar *et al.*, 2003, 2004, 2005). Even though mining has had an influence on the current environmental condition of the river, it is important to emphasize the relevant impact of natural weathering of Río Tinto rocks. The Río Tinto system is proposed as a Mars analogue due to characteristics of the area that result from the interaction among the rock substrate, aquifers, and microorganisms. The mineralogical product of these interactions is a very specific association of iron oxides, oxyhydroxides, and sulfates, typical of acidic environments. Some of these minerals (*e.g.*, hematite, jarosite) have recently been observed in areas of Mars, such as Meridiani Planum (Christensen *et al.*, 2004; Klingelhöfer *et al.*, 2004; Squyres *et al.*, 2004). These mineralogies are important because they indicate processes involving liquid water on the martian surface and therefore are extremely interesting for astrobiology.

During the first 2 years of the MARTE project, conventional wireline drilling equipment obtained two cores of more than 160 meters, each located in a sulfide deposit, and another of around 60 meters in a nearby carboniferous meta-sedimentary formation (Fernández-Remolar *et al.*, 2004, 2005, 2008; Stoker *et al.*, 2004, 2005). Geological and biological characterization of subsurface ecosystems was accomplished (Fernández-Remolar *et al.*, 2008). The sulfide ore showed mineral zoning with depth and development of different habitats depending on the water-table depth and degree of rock fracturing (Fernández-Remolar *et al.*, 2008). Habitats

were portrayed by the presence of some mineral composition and textures, which are indicative of environmental properties such as oxidation state or relative pH of each level (*i.e.*, the oxic/anoxic environment change may be traced by the transformation from ferric to ferrous sulfates). The third year of the MARTE project, and the focus of this paper, was to employ a robotic drilling platform that was remotely operated to simulate a 30-day Mars drilling mission. Details of the MARTE drill system and the automated multi-step processing are in Stoker *et al.* (2008). All prior knowledge of the Río Tinto drilling site was withheld from the science teams, forcing them to rely on data just obtained during the MARTE experiment only for their geological and biological interpretations.

The MARTE experiment was valuable because dry robotic drilling, core sampling, and biological and geological analytical technologies were collectively tested for the first time for potential use on Mars. This paper was synthesized from a cooperative effort between scientists and engineers that examined the subsurface geology of a Mars analogue in the Río Tinto region. This work is divided into three sections, which (i) briefly describe drilling, core retrieval, and borehole inspection procedures; (ii) present the geological analysis of core and borehole material and assess problems encountered with the geological analysis; and (iii) examine lessons learned from this drilling simulation.

Mission Procedures and Instrumentation

The location of the drill site was not revealed to the science teams in order to reduce prejudices about the geological characteristics during the simulation. Previous geological and biological knowledge of the Río Tinto was not taken into account during the data interpretation, as in the same way there would not be any background information at a drill site on Mars. The 30-day mission was divided into two periods. The first half of the mission was commanded by a group located at CAB (Madrid, Spain), and the second half by a group located at NASA Ames (California, USA). Both groups were in contact throughout the mission in order to share information. Both groups used the same protocols for recording and analyzing mission data. An engineering technical group was stationed at the drilling site to ensure proper operation of the drilling platform and to approve or deny drilling or analytical procedures submitted by the science team.

The MARTE drilling platform consists of four components (Stoker *et al.*, 2008), the drilling mechanism, the Core Sampling and Handling System (CSHS), the Remote Science Instrument (RSI) and the Borehole Inspection System (BHIS). The drilling mechanism employs dry rotary cutting techniques, including both carbide drag cutters and crystal diamonds. Cuttings were removed from the drill bit by an auger system. The core was taken off from the core tube and delivered into a clamp automatically for analysis. The drill can capture a maximum of 25 cm of core without core ejection, assuming 100% core recovery.

The RSI is a suite of remote sensing instruments that are used for core analysis and are as follows: ATP luminometer for preliminary life detection (Lightning MVP instrument, BioControl Systems Inc., bio-luminescence, adenosine-5'-triphosphate detector), panoramic camera (Canon Power-

Shot S230; $125 \mu\text{m pixel}^{-1}$) and visible–near infrared (VNIR) imaging spectrometer (Brown *et al.*, 2008), color microscopic imager (Canon EOS-10D; $7 \mu\text{m pixel}^{-1}$), and VNIR point spectrometer (Ocean Optics S2000; 450–1000 nm spectral range) (Sutter *et al.*, 2008).

The CSHS (Stoker *et al.*, 2008) is a suite of equipment that holds the cores, cuts them open, moves them under the remote science instruments for inspection, obtains subsamples from the cores, crushes the samples to powder, transfers the powder to *in situ* instruments, and stores or ejects the cores. The main elements of the CSHS include a set of core clamps, a linear transfer rail, a facing saw, a subsampling saw, a rock crusher, a powdered sample transfer system, and a storage comb. There are nine positions in the CSHS rack for storing cores.

The BHIS can only be deployed when the drill is removed from the borehole and is used to examine the walls of the borehole. The BHIS consists of a panoramic camera (JAI M820, 1 mm pixel^{-1}), microscopic camera (JAI M820, $0.05 \text{ mm} \cdot \text{pixel}$), Raman spectrometer [Jobin Yvon JYV-HE633; laser excitation 633 nm (He-Ne), spectral resolution 10 cm^{-1} , spectral range $200\text{--}3600 \text{ cm}^{-1}$] (Stoker *et al.*, 2008), and a magnetic susceptibility detector (GEOVISTA Magnetic Susceptibility Sonde Range 0–7000 mS/m). The BHIS panoramic camera obtained 20 mm wide images of the borehole wall circumference, while the microscopic camera obtained 14 mm wide images every 90° in azimuth.

Drilling, core handling, and remote sensing operations followed a sequence of processes, which are briefly described as follows (Stoker *et al.*, 2008). (1) Once the drill was placed, the science team sent the first operation plan, which commanded the start of drilling and subsequent placing of cores into the CSHS. (2) Once a core was acquired and placed in the CSHS, it was examined by the RSI for data acquisition and then stored in a rack. (3) Interpretation of the core data by the science team determined how to proceed by either rejecting the core, requesting specific data from the imaging spectrometer, and/or subsampling the core for analysis by the Signs Of Life Detector (SOLID2) instrument. The SOLID2 instrument is a small benchtop unit that uses protein microarray technologies to detect microorganisms as well as their metabolic products (Parro *et al.*, 2008). For biological analysis, the interesting piece of core is extracted robotically using a subsampling saw and then crushed and placed into the SOLID2 instrument. When a core had been thoroughly examined and no further analysis was required, it was ejected from the CSHS in order to free the position for subsequent cores. Before acquiring another core, techniques for sterilizing the core capture mechanism and preventing contamination were applied (Miller *et al.*, 2008).

This paper focuses on the interpretation of the core and borehole wall morphological analysis from the RSI and BHIS panoramic and microscopic imagers. Visible–near infrared (Brown *et al.*, 2008; Sutter *et al.*, 2008), Raman (Stoker *et al.*, 2008), SOLID2 (Parro *et al.*, 2008), and ATP luminometer (Bonaccorsi and Stoker, 2008) data are discussed elsewhere.

Rapid interpretation of the remote sensing data from the core and the borehole, including mineralogy, structure, and feature texture characterization, was essential for making mission decisions, as it would be during a real planetary mission. However, data interpretation pursued the final objective of searching for subsurface life. Any indication of liquid

water, organic matter, life, or potentially favorable habitat was sought. Any evidence in these categories was considered grounds for subsampling of the core and performing detailed inspection with the BHIS in the region where the core was obtained. Cores were often composed of disaggregated fragments, and attempts to sample disaggregated rock were sometimes successful; but the technical group did not prefer this because, most of the time, material was lost during retrieval. Criteria used for selecting core subsamples for biological analysis were, from more to less evident: (a) recognition of any biological morphology, (b) identification of aqueous or biogenic minerals, and (c) appearance of microenvironments such as cavities or open fractures where water could penetrate the rocks. The search for these features was performed using the imaging and spectroscopic data of each core. Morphologies of filaments were often recognized and then sampled. Iron sulfates and oxides from pyrite cast or other cavities were also taken for biological analysis. Images before and after the biological sampling were recorded to confirm that the section of core containing the interesting feature had been sampled.

Data were examined and reported on a tight schedule in order to conduct the experiment following a timetable analogous to a Mars drilling mission. The simulation did not include any delay due to Mars–Earth communication, and the operation was not performed around the clock as is typical in Mars missions. After the discussion of daily results at the end of the day, subsequent operational plans for the next day's activities were submitted to the technical group at the drilling site for approval. Once approved, the technical group converted the science activities request into commands to the drilling mechanism and/or analytical instruments and ensured that operations were performed successfully.

Interpretation of Geology: The Core and the Borehole

A borehole of 5.7 meters was perforated by robotic drilling during the 30-day campaign (Fig. 1). Difficulties encountered in the drilling operations caused by the low mechanical strength of the rock allowed only 35% of the core to be recovered. The remaining 65% of the material was lost because the core capture mechanism had no method for containment of unconsolidated material. Additionally, some of the unconsolidated core material was lost when compressed air was used to assist cuttings transport. Much of the returned core was fragmented and abraded. In many cases, rock fragments from upper levels fell out of the borehole walls and were sampled in lower cores (Bonaccorsi and Stoker, 2008). Compressed air increased the drilling rate and prevented the drill from becoming stuck but decreased the efficiency of obtaining entire cores. Other contaminant remediation techniques from collapses or residual materials retained in some MARTE drill system pieces are summarized in Miller *et al.* (2008).

After the analysis of the cores, it was concluded that the lithology was rather homogeneous and consistent with a typical gossan. Gossan is an intensely oxidized, weathered or decomposed rock, usually from the surface or near-surface zone (above the water table) of a sulfide-rich deposit or mineralized vein. Some mineral compositions and textures characteristic of a gossan, as is predicted to exist in the Río Tinto

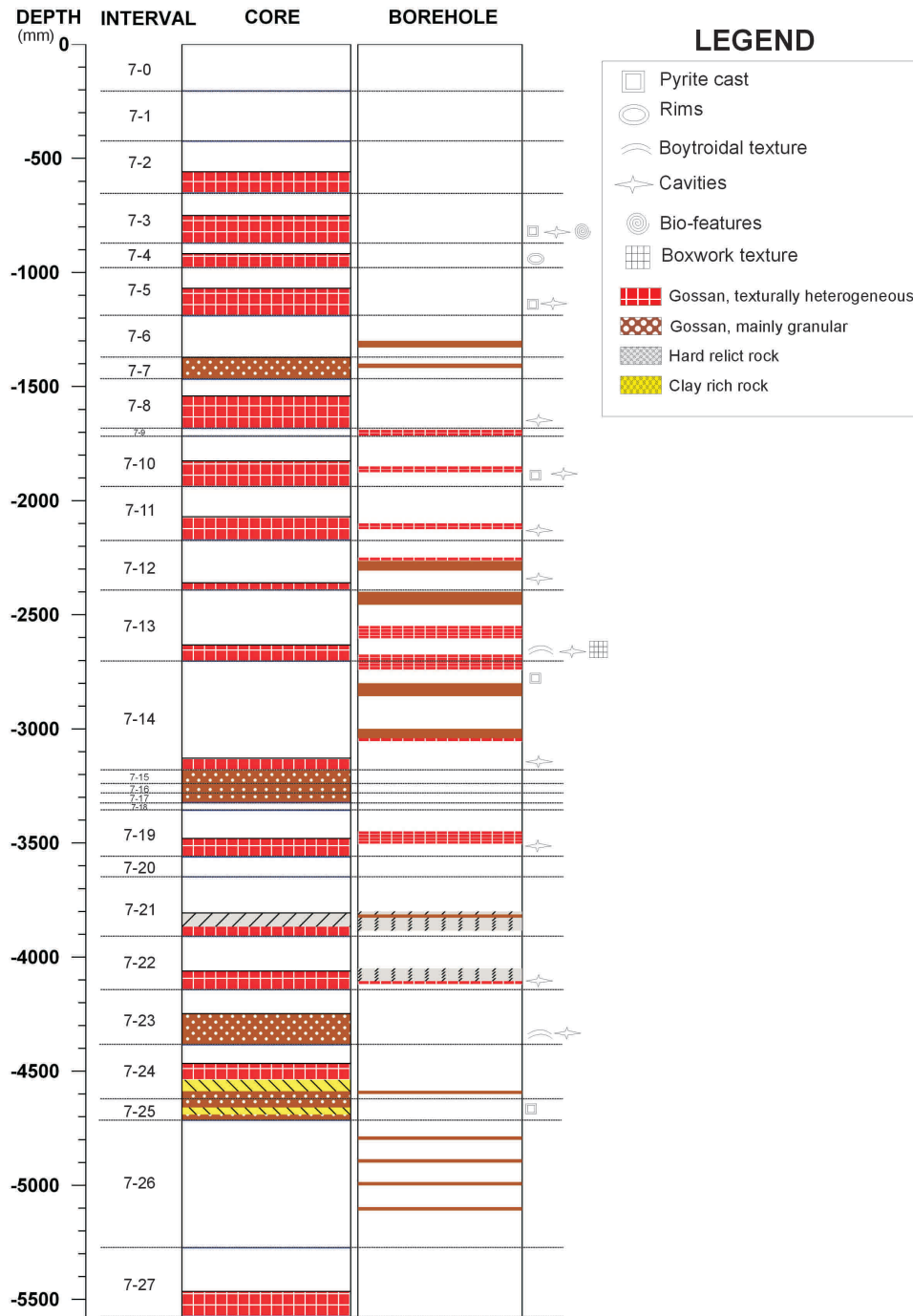


FIG. 1. Stratigraphic column that has been reconstructed from the core and borehole data from drill site 7. White spaces indicate that there are no data from these depths.

area, have been recognized in the cores that were extracted. The drill hole intersected highly oxidized rock, in which original sulfides had been totally dissolved, leaving cavities that were coated by iron oxides and oxyhydroxides such as hematite and/or goethite (Sutter *et al.*, 2008). Sulfide crystals have been replaced by pseudomorphs of iron sulfates or oxides. Other remaining minerals of the gossan were phyllosilicates and quartz, which frequently have distinctive boxwork texture (Fig. 2).

Pseudomorphism indicates that a mineral is altered in such a way that its internal structure and chemical compo-

sition is changed but the characteristic crystal outline of the mineral is preserved. The process of pseudomorphism may be due to mechanical, structural, or chemical changes by three mechanisms: substitution, encrustation, or alteration. In our case, pseudomorphs of secondary minerals (iron oxides and oxyhydroxides) replacing pyrite were observed. Although in some mineral grains of the core samples pseudomorphism is incipient (revealed by the development of alteration rims), normally the alteration of the primary iron sulfides is complete, displaying typically cubic and pyritohedral forms. Botryoidal texture reflects an external arrange-

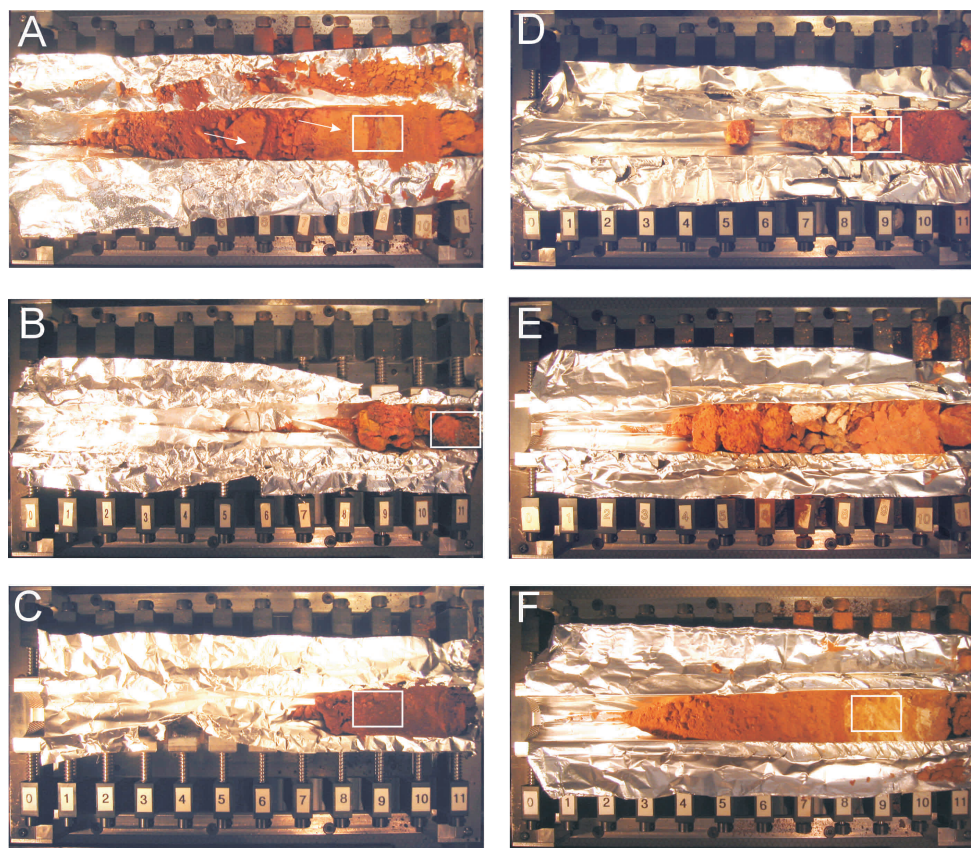


FIG. 2. Examples of the panoramic images from some intervals of the core. Total length of the core storage rack is 25 cm, which is the maximum depth able to be perforated each time. The position of different features and place for subsampling can be indicated by the number on the clamp shown at the bottom part of the picture. The top of the core is in location 0 and the bottom in 11. White rectangles are the intervals shown in Fig. 3. (A) Core 7-3. Perforated interval was from 430 to 650 mm, but just 120 mm were retrieved. The core is not all consolidated, but fragmented in pieces from 4 millimeter to submillimeter. Even at this scale, some cavities in the harder fragments are shown (white arrows). (B) Core 7-11, from the interval between 1949 and 2171 mm depth. The extracted material was 100 mm in six hard pieces. Some pieces have differences in color due to differences in the properties of the oxidized minerals. (C) Core 7-16, perforated just from 3253 to 3291; all the material was retrieved, but it was not able to continue until 250 mm because the borehole wall caved. The material is unconsolidated and has a granular texture. (D) Core 7-21. The interval drilled was from 3653 to 3908, but only 100 mm were taken. Lighter and harder material can be observed on the top part of the core, while reddish disaggregated material is at the bottom. (E) Core 7-23. (F) Core 7-25.

ment, presenting an aggregation of small spheroidal or bulbous prominences, and is one of the most common mineral habits of some secondary minerals [*e.g.*, goethite; Smith and Eggleton (1983)]. This texture implies a genetic processing of the minerals from a gel or colloidal mass. Boxwork texture is defined as a meshwork of porous goethite that remains after much of the original sulfide was leached away (Fig. 3).

Weathering has acted heavily on the material, disaggregating the oxidized rock and producing granular texture in some areas. Recognition of this type of rock was achieved from the interpretation of data from the cores and the borehole, which are described below (Fig. 1).

The core

The beginning of robotic drilling was problematic because the first 500 millimeters (Core 7-1) of the core were not recovered due to the softness and fine-grained nature of the

surface material. Cohesive and recoverable material was first obtained at 515 mm (Core 7-2). Reddish and fragmented angular pieces (7-2; from 430 to 650 mm) were recovered that possessed some surface cavities and were coated by dark microcrystalline minerals, probably goethite.

From 515 to 1174 mm (Cores 7-2 to 7-5), the material was similar, with some softer parts due to the more abundant presence of clays, alternated with other harder patches due to the original rock being richer in quartz. Pyrite casts and irregular cavities filled by brown-red minerals, probably goethite and hematite, were abundant throughout the core (Fig. 2).

After an interval without core recovery (7-6), a pair of cores were obtained (7-7 and 7-8) containing the same reddish material as before but enriched in disaggregated fine-grained minerals. Some patches of yellowish minerals embedded in the orange-oxidized matrix were observed using the Microscopic Imager (data not shown). Color differences

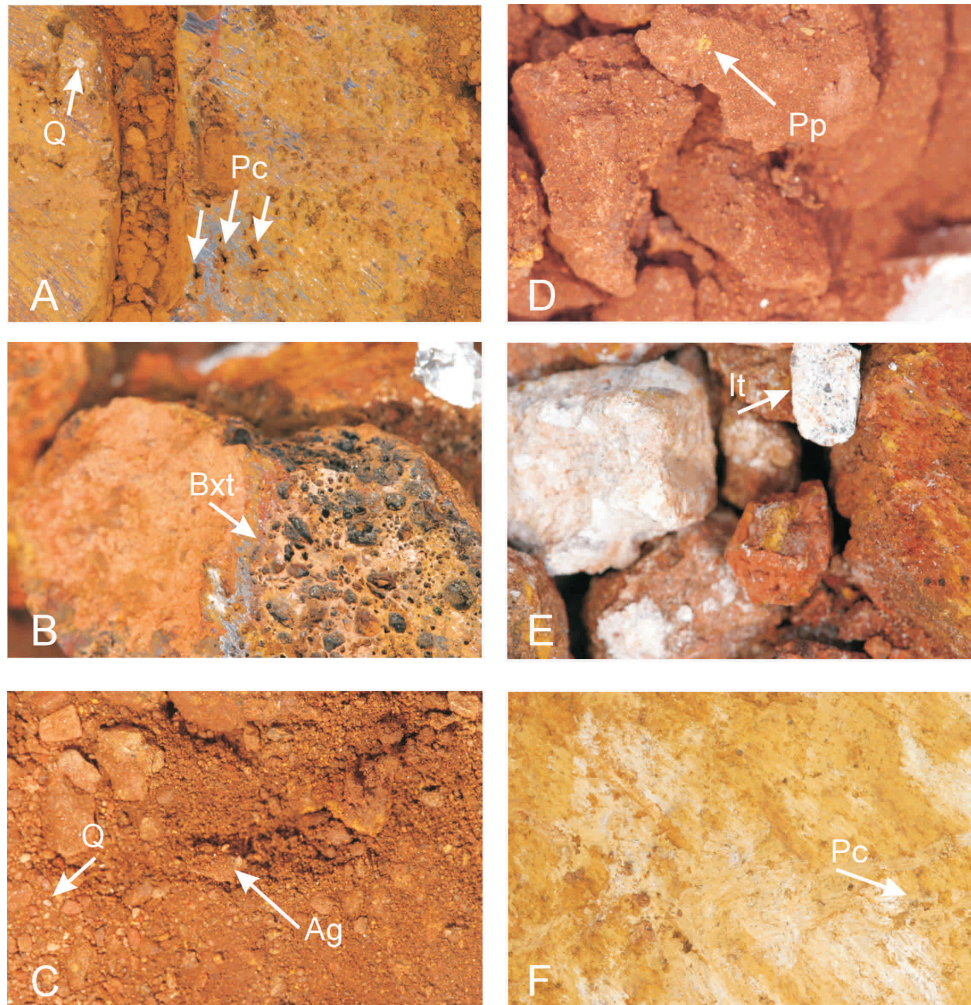


FIG. 3. Microscopic images from different intervals. Each image covers 25×10 mm, with spatial resolution $52 \mu\text{m}/\text{pixel}$. Images are taken automatically at specific positions (45, 85, 125, 165, 205, 245 mm long), but requests for images at specific locations could be made. (A) Core 7-3 at position 205 mm. Image shows two fragments of the harder part of the gossan, where white subrounded quartz grains (Q) persist while pyrite has disappeared, leaving casts coated with oxides (Pc). (B) Image of Core 7-13 at position 205 mm, showing boxwork texture of gossan (Bxt). (C) Core 7-16 at position 205, exhibiting the granular texture that gossan has in many stretches. It is formed by singular grains such as quartz minerals (Q) and aggregates of previous disaggregated oxides, clays, and felsic minerals (Ag). (D) Core 7-15 at position 185 showing angular aggregates of gossan grains and crystals. White arrow points to a pseudomorph of pyrite (Pp). (E) Core 7-21 at position 205, where there are fragments of rock with igneous texture (It), probably relicts of the original andesite where sulfides were injected. (F) Core 7-25 at position 205, where the felsic weathered rock is shown. Some pyritic casts (Pc) are labeled.

indicate either the presence of new minerals because of a change in the stability of the previous minerals, different grain sizes, or changes in crystallinity of the constituent minerals. Iron oxide patches and intergrowths were the most common textures, probably due to secondary mineral replacement.

The unconsolidated and friable nature of the rock at approximately 1700 mm resulted in the loss of Core 7-9. To prevent refilling of the borehole by wall collapse, compressed air was blown down hole to move the cuttings up the auger flights. The use of compressed air was a field solution, initially not included in the MARTE drill system. So the operation was not automatic but manual. This resulted in the loss of the finer grain fractions of the rock and the recovery of a very small amount of core material. However, compressed air was not needed for the harder and cleaner rock fragments

from 1725 to 3180 mm depth (7-10 to 7-14) (Fig. 2). Sometimes core fragments were rotated relative to the short horizontal axis, so the pictures showed the interior of the core. This was taken into account for subsampling purposes because they had anomalous geometry. These fragments were also pyrite cast rich in some places, producing the typical boxwork texture (Fig. 3).

Cores 7-15 to 7-20 (3183 to 3653 mm) were friable and, without compressed air to remove material, fine-grained fractions were again retrieved. Submillimeter granular texture predominated, and subrounded to subangular grains prone to forming agglomerates were observed from the core. Alternating zones of orange/yellowish mineralogies to other more red/brown mineralogies indicate different rates of alteration (Figs. 2 and 3) along the cores because of heterogeneities in the rock.

Lighter-colored material was present from 3835 to 3900 mm (7-21), possibly due to a highly leached felsic/silica-rich part of the ore. The rock texture in 7-21 appeared to be of primary igneous rocks, probably from an original andesite if the felsic mineralogy is also taken into account (Fig. 3). The granular iron oxide-rich material with vugs and quartz crystals in the harder parts of the core appeared again in 7-22 and 7-23 (3900–4388 mm). Some cavities show reddish-pink coatings as well as fractured surfaces. During the mission, zones of lighter-colored areas were proposed to be alteration of tectosilicates to clays such as kaolinite. Post-mission X-ray analysis indicated that the lighter-colored material was dominated by illite, ~3 wt% kaolinite and traces of smectite (Sutter *et al.*, 2008). Yellowish brown materials, probably limonitic, are present in the reddish granular rock in 7-24 and 7-25 (4550 and 4650 mm) (Fig. 3). In the last meter drilled, just 11 cm of material was retrieved. This material was also granular and poorly consolidated, red to yellow iron oxide rich, with minor clays and quartz.

The borehole

The BHIS could only be deployed when the drill was not in the hole. Sometimes the BHIS image analysis was needed to cover areas where core material was lost and sometimes to attempt to correlate interesting features already recognized in the core images. Image adjustments (for the panoramic camera or the microscopic camera) had to be made down hole, including modifying illumination and focusing, because calibration of these systems was not adequate for best results.

Panoramic images were useful for providing context for the BHIS microscopic images and for correlating core panoramic images with borehole wall images. In general, no primary or secondary macroscopic rock structures, such as stratification, nor any clear fracturing patterns were detected along the borehole. Some weathering features of the rock were occasionally resolved in panoramic images; for instance, some heterogeneities in the weathering rate into the gossan were easily observed (Fig. 4). Other characteristics, such as variation in rock hardness, were also identified in some places by observing scratches from the drill bit, and they were associated with the core materials (Fig. 4). We also inferred that images were blurred when the rock walls were friable, implying that material collapsed into the hole.

The resolution of the panoramic camera was not ideally suited for petrological analysis. The needed resolution was achieved by creating image mosaics of the borehole wall with the microscopic camera from interval 7-6 to the bottom. Microscopic camera images show some details from the wall of the borehole, but the interpretation had to be done carefully because frequently some artifacts occurred due to illumination. For instance, subrounded to subangular bright spots from millimeter cavities in the walls seemed to be minerals or cavities but could have been caused by light reflection. Correlation with the core was strongly dependent on the identification of clear features in the borehole microscopic camera images. Wall areas with color differences, preferred mineral orientations, or vestiges of the original rock were sometimes correlated with core material. For example, areas of Core 7-21 (Fig. 2d) enriched in felsic minerals can be observed in BHIS images (Fig. 4c). However, for the most part

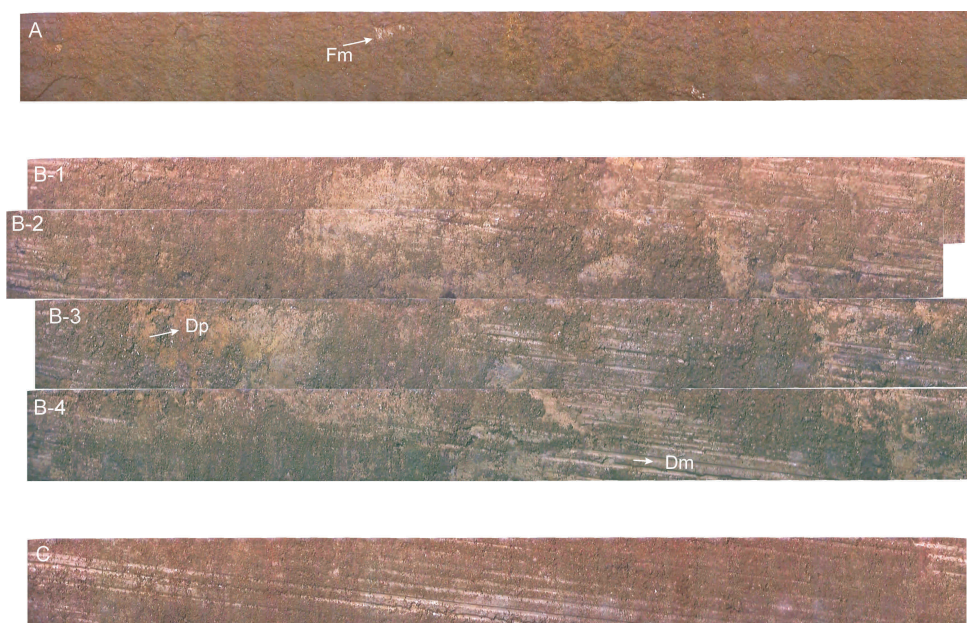


FIG. 4. BHIS images. (A) Panoramic image from the borehole starting at 1864 mm depth to 1884 mm, which corresponds to the 7-10 interval. Global texture of this part of the rock is granular. Some brighter spots probably due to felsic minerals (Fm) can be observed. (B) Overlapping images from 2686 to 2728 mm depth using the microscopic camera in panoramic mode. B-1 and B-2 correspond to Core 7-13; B-3 and B-4 have no associated core. The mosaic displays the heterogeneous structure of the core, with brighter areas probably due to harder and more felsic-rich parts of the rock, and darker areas containing clays and oxides. Drill marks (Dm) are more visible in harder areas. Patches with differences in color (Dp) can be observed. (C) Borehole image from 3842 to 3856 mm depth, which corresponds to interval 7-21. Drill marks on the walls denote harder rock. Core images from this area, showing felsic igneous relicts, can be correlated with brighter parts.

correlating borehole wall features with core material was extremely difficult. Association between features of the images from the cores and inside the borehole are sometimes unclear mainly due to differences in illumination angles and resolution. Furthermore, linking Raman data of borehole wall material with corresponding core material also proved challenging.

Discussion

Even though the drilling site was not known to the science team, finding gossan at Río Tinto was not surprising. This was especially true for the science team from CAB who were familiar with the region and are aware that the Río Tinto is characterized as containing gossan. This made it difficult not to be biased during the geological analysis. Nevertheless, the selected drilling site was appropriated considering the mineralogical analogies between the Río Tinto gossan and an area like Meridiani Planum, Mars.

Only 35% of the core was recovered because of poor competency of the rock and the characteristics of the drilling mechanism (Stoker *et al.*, 2008). A Mars drilling mission may be forced to accommodate conditions of poorly consolidated rock especially if the drilling platform is not mobile. Borehole wall failure, which causes the borehole to fill up and widen as the drilling progresses, was a problem during drilling, especially when drilling through weakly consolidated rock. Borehole infall was minimized by utilizing compressed air; however, this had the side effect of blowing finer materials out the hole, resulting in low core recovery. Correlation between borehole wall and core imaging data should be improved. Sometimes BHIS and RSI data could be correlated, but for the most part such a correlation was difficult or impossible. The absolute position of the core material relative to the borehole wall was not exactly known due to poor core recovery and/or the disturbed nature of the recovered material. When the panoramic imager resolution was determined to be too poor for morphological and petrological interpretations, the microscopic camera was utilized in a mosaicing mode to obtain higher-quality images. Still, images of the borehole wall were often quite featureless, leading to the suspicion that cuttings may coat them. Further tests are needed to verify this. The borehole wall data did have the added benefit of supplementing the core data when core recovery was absent. This suggests that a borehole inspection system would be invaluable during a Mars mission, especially if low core recovery is a problem.

Conclusions

The 2005 simulated robotic drilling mission was instructive in understanding problems associated with dry drilling, core retrieval, and data interpretation that would occur during an actual Mars drilling mission. Drilling reached a depth of 606 cm into ordinary gossan, but not all material was recovered. No new geological information was obtained from examining the gossan at Río Tinto, but useful drilling and procedural experience was obtained from drilling into this analog material.

The imaging instruments used during the mission were useful for defining geological characteristics such as the microgeomorphology, stratigraphy, mineralogy, type of rock alteration, and structure. The instruments provided enough

information for selecting the samples for biological analysis. Sometimes clear biological features like filaments and roots were observed. However, in the absence of unambiguous biomorphologies, the core areas to search for evidences of life were selected by looking for evidence of alteration such as the presence of rock cavities associated with water-related minerals (Fig. 2A). Combined data from the core and the borehole allowed the geologists to complete a stratigraphic description of the borehole. The main gossan minerals identified from the microscopic images were iron oxides, sulfates, and phyllosilicates. Problems encountered during the drilling were mostly attributed to the poorly consolidated nature of the gossan, which contributed to poor core recovery and borehole wall failure that dropped upper wall material onto the lower cores. Despite these problems, flexible drilling, sampling, and analytical protocols during the mission and constant communication between the scientific and technical groups improved science results. Lessons learned from this work can be applied to developing drilling and instrument technologies that will be used for future Mars drilling missions.

Abbreviations

ATP, adenosine-5'-triphosphate; BHIS, Borehole Inspection System; CAB, Centro de Astrobiología; CSHS, Core Sampling and Handling System; MARTE, Mars Astrobiology Research and Technology Experiment; RSI, Remote Science Instrument; SOLID2, Signs Of Life Detector; VNIR, visible-near infrared.

References

- Bonaccorsi, R. and Stoker, C.R. (2008) Science results from a Mars drilling simulation (Río Tinto, Spain) and ground truth for remote science observations. *Astrobiology* 8:967–985.
- Boulter, C.A., Hopkins, L.J., Ineson, M.G., and Brockwell, J.S. (2004) Provenance and geochemistry of sedimentary components in the Volcano-Sedimentary Complex, Iberian pyrite belt: discrimination between the sill-sediment-complex and volcanic-pile models. *J. Geol. Soc. London* 161:103–115.
- Brown, A.J., Sutter, B., and Dunagan, S.E. (2008) The MARTE VNIR Imaging Spectrometer experiment: design and analysis. *Astrobiology* 8:1001–1011.
- Christensen, P.R., Wyatt, M.B., Glotch, T.D., Rogers, A.D., Anwar, S., Arvidson, R.E., Bandfield, J.L., Blaney, D.L., Budney, C., Calvin, W.M., Fallacaro, A., Ferguson, R.L., Gorelick, N., Graff, T.G., Hamilton, V.E., Hayes, A.G., Johnson, J.R., Knudson, A.T., McSween, H.Y., Jr., Mehall, G.L., Mehall, L.K., Moresch, J.E., Morris, R.V., Smith, M.D., Squyres, S.W., Ruff, S.W., and Wolff, M.J. (2004) Mineralogy at Meridiani Planum from the Mini-TES experiment on the Opportunity Rover. *Science* 306:1733–1739.
- Fernández-Remolar, D.C., Rodríguez, N., Gómez, F., and Amils, R. (2003) Geological record of an acidic environment driven by iron hydrochemistry: the Tinto River system. *J. Geophys. Res.* 108, doi:10.1029/2002JE001918.
- Fernández-Remolar, D., Gómez-Elvira, J., Gómez, F., Sebastian, E., Martin, J., Manfredi, J.A., Torres, J., Kesler, C.G., and Amils, R. (2004) The Tinto River, an extreme acidic environment under control of iron, as an analog of the Terra Meridiani hematite site of Mars. *Planet. Space Sci.* 52:239–248.
- Fernández-Remolar, D.C., Morris, R.V., Gruener, J.E., Amils, R., and Knoll, A.H. (2005) The Río Tinto basin, Spain: mineral-

- ogy, sedimentary geobiology, and implications for interpretation of outcrop rocks at Meridiani Planum, Mars. *Earth Planet. Sci. Lett.* 240:149–167.
- Fernández-Remolar, D.C., Prieto-Ballesteros, O., Rodríguez, N., Gómez, F., Amils, R., Gómez-Elvira, J., and Stoker, C.R. (2008) Underground habitats in the Río Tinto Basin: a model for subsurface life habitats on Mars. *Astrobiology* 8:1023–1047.
- Klein, H.P. (1979) The Viking mission and the search for life on Mars. *Rev. Geophys.* 17:1655–1662.
- Klingelhöfer, G., Morris, R.V., Bernhardt, B., Schroder, C., Rodionov, D.S., de Souza, P.A., Yen, A., Gellert, R., Evlanov, E.N., Zubkov, B., Foh, J., Bonnes, U., Kankeleit, E., Gutlich, P., Ming, D.W., Renz, F., Wdowiak, T., Squyres, S.W., and Arvidson, R.E. (2004) Jarosite and hematite at Meridiani Planum from Opportunity's Mössbauer spectrometer. *Science* 306:1740–1745.
- Leistel, J.M., Marcoux, E., Thieblemont, D., Quesada, C., Sanchez, A., Almodovar, G.R., Pascual, E., and Sáez, R. (1998) The volcanic-hosted massive sulphide deposits of the Iberian Pyrite Belt—review and preface to the thematic issue. *Mineralium Deposita* 33:2–30.
- Miller, D.P., Bonaccorsi, R., and Davis, K. (2008) Design and practices for use of automated drilling and sample handling in MARTE while minimizing terrestrial and cross contamination. *Astrobiology* 8:947–965.
- Moreno, C. (1993) Postvolcanic paleozoic of the Iberian Pyrite belt—an example of basin morphologic control on sediment distribution in a turbidite basin. *J. Sediment. Petrol.* 63:1118–1128.
- Parro, V., Fernández-Calvo, P., Rodríguez Manfredi, J.A., Moreno-Paz, M., Rivas, L.A., García-Villadangos, M., Bonaccorsi, R., González-Pastor, J.E., Prieto-Ballesteros, O., Schuerger, A.C., Davidson, M., Gómez-Elvira, J., and Stoker, C.R. (2008) SOLID2: an antibody array-based life-detector instrument in a Mars drilling simulation experiment (MARTE). *Astrobiology* 8:987–999.
- Smith, K.L. and Eggleton, R.A. (1983) Botryoidal goethite—a transmission electron microscope study. *Clays Clay Miner.* 31:392–396.
- Squyres, S.W., Grotzinger, J.P., Arvidson, R.E., Bell, J.F., Calvin, W., Christensen, P.R., Clark, B.C., Crisp, J.A., Farrand, W.H., Herkenhoff, K.E., Johnson, J.R., Klingelhöfer, G., Knoll, A.H., McLennan, S.M., McSween, H.Y., Morris, R.V., Rice, J.W., Rieder, R., and Soderblom, L.A. (2004) *in situ* evidence for an ancient aqueous environment at Meridiani Planum, Mars. *Science* 306:1709–1714.
- Stoker, C.R., Dunagan, S., Stevens, T., Amils, R., Gómez-Elvira, J., Fernández, D., Hall, J., Lynch, K., Cannon, H., Zavaleta, J., Glass, B., and Lemke, L. (2004) Mars Analog Río Tinto Experiment (MARTE): 2003 drilling campaign to search for a subsurface biosphere at Río Tinto, Spain [abstract 2025]. In *35th Lunar and Planetary Science Conference*, Lunar and Planetary Institute, Houston.
- Stoker, C.R., Stevens, T., Amils, R., Gómez-Elvira, J., Rodríguez, N., Gomez, F., Gonzales-Torri, E., Aguilera, A., Fernández-Remolar, D., Dunagan, S., Lemke, L., Zavaleta, J., and Sanz, J.L. (2005) Characterization of a subsurface biosphere in a massive sulfide deposit at Río Tinto, Spain: implications for extant life on Mars [abstract 1534]. In *36th Lunar and Planetary Science Conference*, Lunar and Planetary Institute, Houston.
- Stoker, C.R., Cannon, H.N., Dunagan, S.E., Lemke, L.G., Glass, B.J., Miller, D., Gomez-Elvira, J., Davis, K., Zavaleta, J., Winterholler, A., Roman, M., Rodriguez-Manfredi, J.A., Bonaccorsi, R., Bell, M.S., Brown, A., Battler, M., Chen, B., Cooper, G., Davidson, M., Fernández-Remolar, D., Gonzales-Pastor, E., Heldmann, J.L., Martínez-Frías, J., Parro, V., Prieto-Ballesteros, O., Sutter, B., Schuerger, A.C., Schutt, J., and Rull, F. (2008) The 2005 MARTE robotic drilling experiment in Río Tinto, Spain: objectives, approach, and results of a simulated mission to search for life in the martian subsurface. *Astrobiology* 8:921–945.
- Sutter, B., Brown, A., and Stoker, C.R. (2008) Visible-near infrared spectrometry of drill core samples from Río Tinto, Spain: results from the 2005 Mars Astrobiology Research and Technology Experiment (MARTE) drilling exercise. *Astrobiology* 8:1049–1060.
- Tornos, F. (2006) Environment of formation and styles of volcanogenic massive sulfides: the Iberian Pyrite Belt. *Ore Geology Reviews* 28:259–307.
- Zent, A.P. and McKay, C.P., (1994) The chemical reactivity of the martian soil and implications for future missions. *Icarus* 108:146–157.

Address reprint requests to:

Olga Prieto-Ballesteros
 Centro de Astrobiología-INTA-CSIC
 Carretera de Ajalvir km. 4
 Torrejón de Ardoz
 28850 Madrid
 Spain

E-mail: prietobo@inta.es